3rd China-Japan Joint Workshop on Positron Science (JWPS2017)
JJAP Conf. Proc. **7**, 011101 (2018) https://doi.org/10.7567/JJAPCP.7.011101

Effect of Beam Flux on Radiation Damage Accumulation in Ion-bombarded Si

Hideaki Minagawa[1], Shunsuke Nakanishi[1], Masaki Maekawa[3], Atsuo Kawasuso[3], and Hidetsugu Tsuchida[1*,2]

[1]*Department of Nuclear Engineering, Kyoto University, Nishikyo-ku, Kyoto 615–8530, Japan*
[2]*Quantum Science and Engineering Center, Kyoto University, Uji, Kyoto 611–0011, Japan*
[3]*National Institute for Quantum and Radiological Science and Technology (QST), Takasaki, Gumma 370–1292, Japan*

E-mail: tsuchida@nucleng.kyoto-u.ac.jp

(Received November 1, 2017)

The effects of ion flux on radiation defect production are studied for single crystal silicon bombarded by 6.7 MeV carbon ions. The resultant damage was characterized by X-ray diffraction analysis and positron annihilation Doppler broadening spectroscopy. The results showed that lattice shrinkage occurs after irradiation although the amount of shrinkage decreases with increasing flux at a fixed fluence. This implies that defect concentration is decreased at higher flux. The major defect is identified as a divacancy. To evaluate this flux effect, we consider the flux dependence of defect recombination by defect reaction rate theory. The calculation suggests that the experimental results can be explained by considering the flux effect on the defect recombination process except thermal annealing. This suggests that the reaction rate constant varies by ion flux i.e., the rate of displacements per atom.

1. Introduction

Ion irradiation-induced damage evolution in crystalline materials has been extensively studied in semiconductor applications of ion implantation [1]. Recent investigations have focused on an understanding of defect relaxation processes (dynamic annealing), demonstrating that damage structures depend on ion flux as well as fluence [2, 3]. The flux effect is caused by the following two processes: (1) thermal effect resulting from beam heating, and (2) non-thermal effect due to spontaneous defect reaction. The damage evolution proceeds by the reciprocal processes of damage production and relaxation in the damage region created along the ion trajectory (ion track).

For Si materials, studies on the flux dependence of defect production have been performed by various damage analysis methods [2, 4, 5]. Hallén et al. [4] studied production of vacancy defects during irradiation at a very low flux by deep-level transient spectroscopy (in this case, the atomic displacement damage rate was on the order of 10^{-12} dpa s^{-1}–10^{-9} dpa s^{-1}), showing that the amount of defects decreases with increasing flux under conditions for non-interference between neighboring ion tracks. This is attributed to the rapidly diffusing silicon interstitials, which overlap the vacancy distributions produced in adjacent ion tracks. Carter and Titov [3,5] investigated amorphization during irradiation at high flux (10^{-4} dpa s^{-1}–10^{-2} dpa s^{-1}) using Rutherford backscattering spectroscopy combined with the ion channeling method. With increasing flux, the lattice microstructure is damaged by multiple overlapping cascades. Thus, the resultant damage structure varies with the intensity of ion flux and the dynamic behavior of interstitials plays an important role in determination of the final damage states.

In this work, we have studied the effect of ion flux on defect accumulation by two defect analysis methods: X-ray diffraction (XRD) and positron annihilation spectroscopy (PAS). XRD analysis enables the characterization of structural changes in crystalline materials. PAS analysis enables the

characterization of open-volume defects including atomic vacancies. The purpose of this study is to understand the mechanism of the recombination of radiation damage and its irradiation parameter dependence. A free-standing, single crystal Si foil is irradiated with MeV-energy carbon ions in the flux range 1.0×10^{13} cm^{-2} s^{-1}–3.0×10^{13} cm^{-2} s^{-1} (the corresponding dpa rate were 2.5×10^{-4} dpa s^{-1}–7.4×10^{-4} dpa s^{-1}). We show experimental results of changes of the lattice parameter as a function of ion flux. From a simple model calculation based on reaction rate theory, the flux dependence of the rate constant of defect recombination is discussed.

2. Experiment

Ion irradiation experiments were performed using a 1.7 MV Cockcroft-Walton-type tandem accelerator at the Quantum Science and Engineering Center, Kyoto University. Target specimens were single crystal Si wafers with a thickness of 12 μm. Projectile beams were 6.7 MeV C ions. The beams were well collimated to have a uniform intensity distribution and a spot size of 1.5 mm in diameter. The range of the projectile was approximately half of the wafer thickness, so the defect concentration maximizes at the center of the target depth. A free-standing Si wafer was irradiated at three different ion fluxes (1.0×10^{13} cm^{-2} s^{-1}, 2.0×10^{13} cm^{-2} s^{-1}, and 3.0×10^{13} cm^{-2} s^{-1}) to a fixed fluence of 1.0×10^{16} cm^{-2}. The resultant damage was investigated in terms of a change in the lattice parameter, and type of defects.

Lattice parameter measurements were performed using the X-ray diffraction method. Details of the measurements were described in a previous study [6]. Briefly, the apparatus consists of a conventional point-focusing diffractometer (RINT 2000, Rigaku Co. Japan), which was operated at 0.9 kW (30 kV, 30 mA) for Cu K radiation to obtain a highly intense X-ray microprobe. The X-ray beam was collimated to a spot size of 0.5 mm in diameter. The X-ray incident angle θ was 34.0° to 35.0° because XRD spectra were taken at 2θ diffraction angles from 68.0° to 70.0° and XRD scanning was performed in the $2\theta/\theta$ scan mode, i.e., the X-ray incident angle was changed by rotating the target to keep the incident angle to the target surface equal to the reflection angle during a scan. The beam spot on the target has an elliptical shape (the minor and maximum major radii of the ellipse were 0.5 mm and 0.9 mm, respectively). Thus, the X-ray beam was incident within the ion-irradiation area. XRD spectra were taken with a step interval of 0.01° and a scanning rate of 0.5 s per step. In each diffraction spectrum measurement, the total time to collect data was 100 s, according to the scanning rate and scanning range. To keep good counting statistics, the total count in the diffraction peak area was $\geq 10^5$. The overall experimental uncertainty for lattice parameter measurements arising from the limitation of the parallel slit analyzer opening angle (0.005°) was $\pm 6 \times 10^{-5}$ or less.

Analysis of defect species was performed by positron beam Doppler broadening annihilation spectroscopy. The measurements were conducted using the ^{22}Na RI-based high-intensity, slow positron beam apparatus equipped with a solid Ne moderator at the National Institute for Quantum and Radiological Science and Technology (QST), Takasaki, Japan. According to a TRIM calculation, the damage distribution for 6.7-MeV C in Si has a peak at a sample depth of approximately 5.5 μm. The positron beam was focused to a spot size of 1.0 mm in diameter by a magnetic lens. To overlap the damage region with the positron probing region, the positron implantation energy was set to 35 keV, where the corresponding mean depth was 5.0 μm. The annihilation γ-ray was detected by a high-purity germanium semiconductor detector. The photo-peak spectrum was characterized by the low- and high-momentum line shape parameters S and W, defined as the ratio of the counts in the central region (from 510.3 keV to 511.7 keV) and the wing regions (from 505.9 keV to 508.2 keV and 513.8 keV to 516.1 keV) of the annihilation photo-peak to the total counts in the peak (from 504.6 keV to 517.4 keV), respectively.

3. Results and Discussion

To study the flux effect on lattice parameter change, we performed XRD analysis and measured the change in the Si(400) diffraction peak observed before and after irradiation. The peak position observed for an un-irradiated specimen was around $2\theta = 69.134°$, corresponding to a lattice parameter (a_0) of 5.432 Å. This is in good agreement with the standard value of 5.431 Å for single crystal Si [7] within the experimental uncertainty. In the estimation using Bragg's rule, we took the wavelength of the incident X-ray (Cu Kα) as 1.541 Å. The peak positon observed after irradiation was shifted to higher angle, indicating lattice shrinkage. In addition, its peak shape was almost unchanged and no change in the XRD pattern in a wide range $2\theta = 30°$–$80°$ was observed. This suggests no significant damage including large voids or dislocation loops.

The effect of ion flux on relative changes in lattice parameter, defined as $\Delta a/a_0 = (a - a_0)/a_0$, where a_0 and a are lattice parameters obtained before and after irradiation, was examined. Figure 1 shows $-\Delta a/a_0$ as a function of flux, where the total fluence was fixed to 1×10^{16} cm^{-2} for each flux. $-\Delta a/a_0$ decreases with increasing flux. This implies that the amount of defects is reduced by the annealing effect with increasing flux.

To identify the accumulated defect species, we performed Doppler broadening of e^+-e^- annihilation radiation (DBAR) measurements for the same specimens used in the XRD analysis. Figure 2 shows the flux dependence of the annihilation line parameter S or W normalized to that measured for the un-irradiated specimen ($S_0 = 0.5035 \pm 0.0005$, $W_0 = 0.0194 \pm 0.0001$). The S parameter is increased by approximately 2.5 % for the Si irradiated with a flux of 1.0×10^{13} cm^{-2} s^{-1} and decreases with increasing flux. This behavior is similar to that shown in the XRD results. According to calculations by Hakala et al. [8], the S parameter increases after formation of mono-vacancy and divacancy by 1.8 % and 4.5 %, respectively. Those calculations are comparable to the present results, but quantitatively different. This difference is considered to be due to the following factors. In the DBAR measurements, all of the positrons were not trapped into ion-induced defects owing to non-uniform ion-damage distributions along the target depth. The damage may consist of a mixture of different types of defects, i.e., mono-vacancy and divacancy. Another factor may result from influence of the ion implantation (the projectile beam investigated was carbon). The S parameter is reduced by positron annihilation with the implanted carbon atoms. The observed W parameter is larger than the calculation in Ref. 10, and this is probably caused by the influence of carbon atoms.

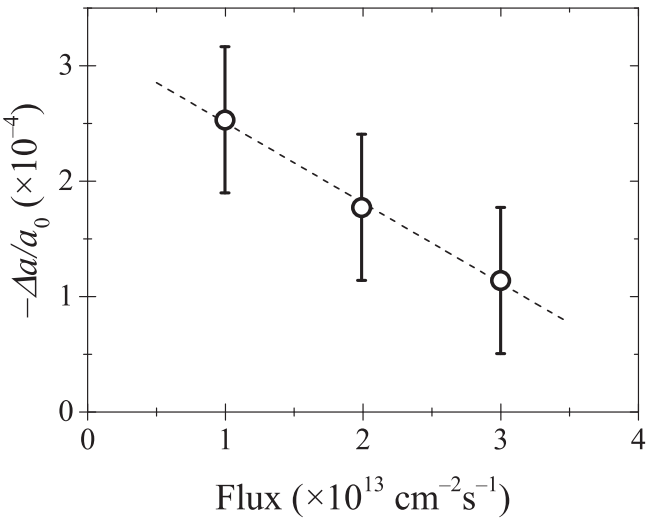

Fig. 1 Flux dependence of relative changes in lattice parameter $\Delta a/a_0$. The total fluence was fixed to 1×10^{16} cm^{-2} for each flux.

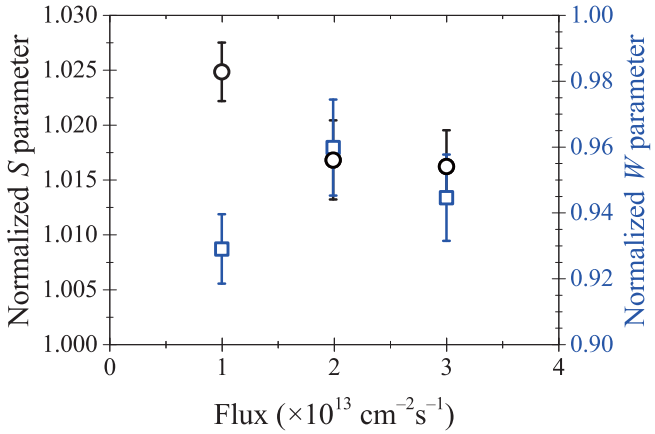

Fig. 2 Flux dependence of S or W parameter normalized to that measured for un-irradiated specimen. The symbols ○ and □ denote S and W parameters, respectively. Total fluence was 1×10^{16} cm^{-2} for each flux. All of the data are obtained from the same samples used in XRD measurements.

Accumulation of these defects induces lattice expansion or shrinkage. Namely, vacancy sites cause the host lattice to shrink, whereas interstitial sites cause the host lattice to expand. In the latter, an interstitial site has a dumbbell structure. Assuming isotropic volume changes, the relationship between lattice parameter change and volume change is

$$\left(1 + \frac{\Delta a}{a_0}\right)^3 = 1 + \frac{\Delta V}{V_0}\,, \tag{1}$$

where V_0 is the original volume and $\Delta V = nV^{\mathrm{rel}}$ with the number of defects n and the relaxation volume associated with defects V^{rel}. The concentration of defects is expressed as $C = n\Omega/V_0$, where Ω is the atomic volume. For $|\Delta a/a_0| \ll 1$, $\Delta a/a_0$ is given by

$$\frac{\Delta a}{a_0} = V^{\mathrm{rel}} \times \frac{C}{3\Omega}\,. \tag{2}$$

The XRD and DBAR results showed that the lattice parameter changes are caused by the accumulation of the following defect species: mono-vacancy (V), mono-interstitial (I), and divacancy (V_2). To quantitatively evaluate the flux dependence of lattice parameter changes, we consider the following model. This model is based on the assumptions that ion irradiation produces only a vacancy-interstitial pair and migration of mono-vacancies is the dominant reaction process. According to the results reported in Refs. 9,10, the value of the diffusion coefficient for mono-vacancies (D_V) is considerably larger compared with that for mono-interstitial or divacancy ($D_V/D_{I,V_2} \sim 10^6$). This implies that the dominant recombination is between vacancies and interstitials. According to the reaction kinetics [11], the rate of the change in the defect concentrations C_I, C_V, and C_{V_2} is given by

$$\begin{aligned}
\frac{\mathrm{d}}{\mathrm{d}t}C_V &= \sigma_{\mathrm{d}}\phi - K_{IV}C_IC_V - K_{VV}C_V^2 \\
\frac{\mathrm{d}}{\mathrm{d}t}C_{V_2} &= K_{VV}C_V^2 \\
\frac{\mathrm{d}}{\mathrm{d}t}C_I &= \sigma_{\mathrm{d}}\phi - K_{IV}C_IC_V\,,
\end{aligned} \tag{3}$$

where σ_{d} is the displacement cross section and ϕ is the flux. The value of σ_{d} is estimated as 2.5×10^{-17} cm^2 based on a model described in Ref. 12 and the TRIM code [13], where the displacement energy is taken as 15 eV. K_{IV} and K_{VV} are the reaction rate constants for vacancy-interstitial

recombination and vacancy agglomeration, respectively. By solving Eq. (3) using a numerical analysis, we determined the accumulated defect concentration for a certain irradiation time. Thus, C_I, C_V, and C_{V_2} as a function of fluence Φ were obtained with the relation: $\Phi = \phi \times t$ with ϕ the ion flux and t the irradiation time. The lattice parameter change associated with the defect accumulation, $\Delta a/a_0$, can be obtained by substituting the calculated C_I, C_V, and C_{V_2} into Eq. (2). The relaxation volume was taken as $V_V^{\mathrm{rel}} = -0.25\Omega$ for mono-vacancy [14] and $V_{V_2}^{\mathrm{rel}} = -0.38\Omega$ for divacancy [15], where these nagative values indicate that the formation of these defects leads to lattice shrinkage. The value of V_I^{rel} was obtaned as follows. The relaxation volume of vacanvy-interstitial defects (Frenkel pairs) is expressed as [16]

$$V_{\mathrm{Frenkel}}^{\mathrm{rel}} = V_I^{\mathrm{rel}} + V_V^{\mathrm{rel}} = -0.07\Omega\,,$$

so that V_I^{rel} ($= V_{\mathrm{Frenkel}}^{\mathrm{rel}} - V_V^{\mathrm{rel}}$) is obtained as 0.18Ω. Then, the total lattice parameter change, which corresponds to lattice shrinkage, is given by

$$-\left.\frac{\Delta a}{a_0}\right|_{\mathrm{total}} = \frac{0.25C_V + 0.38C_{V_2} - 0.18C_I}{3}\,.$$

We also consider the influence of carbon implatation on the lattice parameter change. Baker et al. [17] reported that the change in lattice parameter of Si caused by the presence of carbon atoms is the

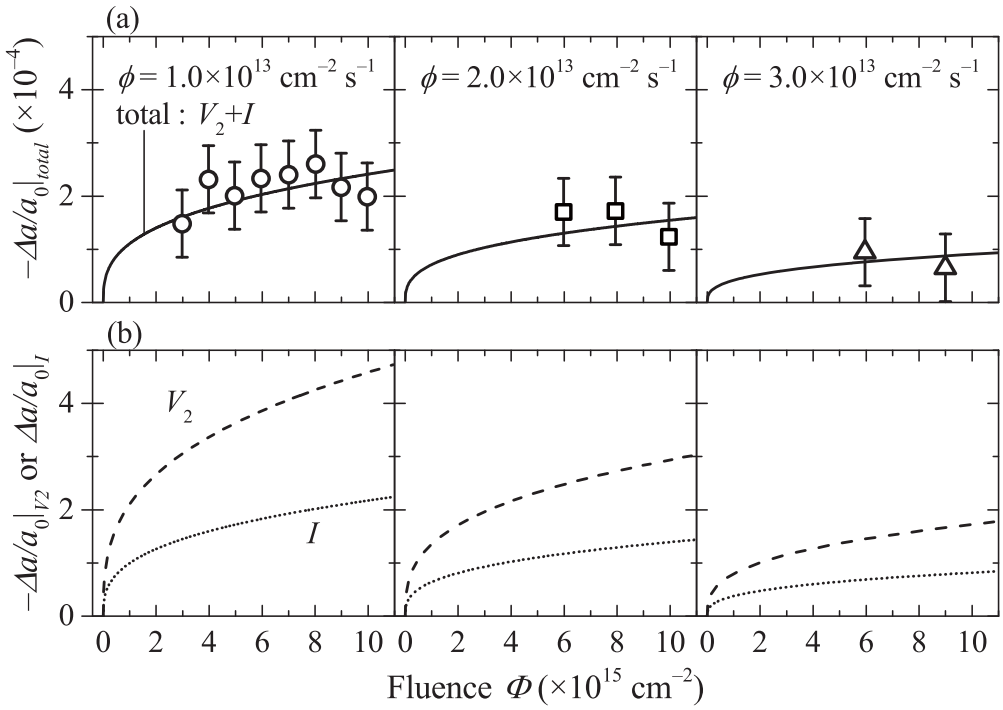

Fig. 3 (a) Fluence dependence of the total lattice parameter change ($-\Delta a/a_0|_{\mathrm{total}}$) caused by defect accumulation, where negative or positive sign for $\Delta a/a_0$ indicates lattice shrinkage or expansion, respectively. Symbols denote experimental data: ○ for 1.0×10^{13} cm^{-2} s^{-1}, □ for 2.0×10^{13} cm^{-2} s^{-1}, and △ for 3.0×10^{13} cm^{-2} s^{-1}. Solid curves denote the results of fitting the data by Eqs. (2) and (3). (b) Dashed and dotted curves indicate the model calculation for lattice parameter change associated with the formation of divacancies ($-\Delta a/a_0|_{V_2}$) and mono-interstitials ($\Delta a/a_0|_I$), respectively.

following relation:

$$-\frac{\Delta a}{a_0}\Big|_{\mathrm{c}} = -6.5 \times 10^{-24} n_{\mathrm{c}} \,,$$

where n_{c} is the carbon concentration (cm^{-3}). The negative sign means lattice shrinkage with increasing n_{c}. We assume that this lattice parameter change occurs over all of the carbon-implanted area including the target thickness. The n_{c} is given by Φ/L, where Φ is the fluence and L is the target thickness. Figure 3 plots $-\Delta a/a_0|_{\mathrm{total}}$ as a fuction of ion fluence for each flux, where symbols denote the experimental data obtained by subtracting the lattice change caused by carbon implantation ($\Delta a/a_0|_{\mathrm{c}}$), and solid curves indicate the result of fitting the data. In addition, in Fig. 3(b) the components for divacancies ($-\Delta a/a_0|_{V_2}$) and mono-interstitials ($\Delta a/a_0|_I$) are marked by the dashed and dotted curves, respectively. The component for mono-vacancies is negligible because of extremely low concentration and no-contribution to the lattice parameter change. We treated the reaction rate constant K_{IV} or K_{VV} as a fitting parameter. Obtained fitting values of K_{IV} and K_{VV} are listed in Table I. The measured value of $\Delta a/a_0|_{\mathrm{total}}$ increases with ion fluence, and then approaches a constant value at higher fluence. Interestingly, the value of K_{IV} increased with flux, suggesting that the rate of recombination of Frenkel pairs is increased with increasing flux. In contrast, K_{VV} has a weak flux dependence. This weak dependence is attributed to the production rate of divacancy (vacancy-vacancy coupling), in which the concentration of divacancy C_{V_2} is decreased because the concentration of mono-vacancy C_V is decreased by increasing the recombination rate. These flux effects can be explained by the following two recombination processes: (1) the thermal effect and (2) non-thermal effect. These effects are closely related to the reaction rate constant K, where K_{AB} denotes defect reaction between defects A and B, and is given by

$$K_{AB} = \frac{z_{AB}\,(D_A + D_B)}{a^2}$$

with a the lattice parameter, D_A or D_B the diffusion coefficient for defect A or B, and z_{AB} the combinatorial factor. The parameter D is influenced by the temperature, and is given by $D = D_0 \exp(-E_{\mathrm{m}}/kT)$, where D_0 is a constant, E_{m} is the migration energy, k is the Boltzmann constant, and T is the target temperature. The values of D_0 for interstitial and vacancy defects are 2.4×10^{-1} $\mathrm{cm}^{-2}\,\mathrm{s}^{-1}$ and 1.3×10^{-3} $\mathrm{cm}^2\,\mathrm{s}^{-1}$, respectively. E_{m} for interstitial and vacancy defects are 0.94 eV and 0.46 eV, respectively [9]. We determined T from the measurements in beam spot area during irradiation by a thermocouple. The measured values of T were 344 K, 388 K, and 424 K for an ion flux of 1.0×10^{13} $\mathrm{cm}^{-2}\,\mathrm{s}^{-1}$, 2.0×10^{13} $\mathrm{cm}^{-2}\,\mathrm{s}^{-1}$, and 3.0×10^{13} $\mathrm{cm}^{-2}\,\mathrm{s}^{-1}$, respectively.

The parameter D is related to the thermal recombination process. On the other hand, the parameter z_{AB} corresponds to the number of recombination sites and does not depend on temperature. This parameter is related to the non-thermal recombination process, i.e., the spontaneous defect reaction.

Table I Fitting parameters: K is the reaction rate constant, z_{IV} and z_{VV} are the combinatorial factor for vacancy-interstitial recombination and vacancy-vacancy agglomeration, respectively.

Flux [10^{13} $\mathrm{cm}^{-2}\,\mathrm{s}^{-1}$]	K_{IV} [10^6 s^{-1}]	K_{VV} [10^7 s^{-1}]	z_{IV}	z_{VV}
1.0	1.8	3.3	20	89
2.0	5.5	3.9	11	19
3.0	15	3.9	9.2	6.0

For the nearest neighbor site in diamond-structured Si, the value of z_{IV} and z_{VV} are 4 and 6, respectively. As shown in Table I, values of z_{IV} and z_{VV} obtained by fitting the data are considerably larger than the values mentioned above. This comparison implies that spontaneous defect reactions occur in a wider range relevant to the nearest neighbor site, i.e., the capture radius in the spontaneous reaction between defects becomes large compared with the nearest neighbor distance. The large value of z_{IV} is attributed to an attractive force between Frenkel pairs induced by virtue of their strain fields [11]. The present results suggest that a similar strain field attracts mono-vacancies with each other. It should be noted that the obtained z_{IV} and z_{VV} decrease with increasing flux. This indicates reduction of the capture radius at higher flux. This behavior is different from that for the thermal effect. The possible mechanism is that the distance between defects produced by irradiation becomes short because higher flux irradiation induces a high density defect. The flux dependence of z_{VV} is stronger than that of z_{IV}, suggesting an active reaction between mono-vacancies rather than mono-interstitials under the present irradiation condition. We conclude that the effect of ion flux on radiation damage in Si materials is attributed to the spontaneous defect reaction. This finding could be useful for evaluation of damage states in the fields of radiation with various intensities.

4. Conclusion

We investigated the flux dependence of lattice parameter changes associated with defect accumulation in single crystal Si by fast-ion irradiation to a fixed fluence. The accumulated defects were characterized by X-ray diffraction analysis and positron annihilation Doppler broadening spectroscopy. We found that the lattice shrinkage is caused by production of divacancies having a negative value of the relaxation volume, and the amount of the shrinkage is decreased with increasing flux. A model calculation showed that the reaction rate constant is increased by the thermal effect resulting from beam heating. In contrast, its value is decreased by the non-thermal effect relevant to spontaneous defect reaction. These effects imply that a parameter such as the combinatorial factor including the reaction rate constant varies by ion flux. Namely, the capture radius for the spontaneous defect reaction becomes large relative to the nearest neighbor distance and it decreases with increasing flux. We conclude that the combinatorial factor is a key parameter to understand the flux effect on radiation damage in materials.

Acknowledgment

We acknowledge Manabu Saito, Makoto Imai, and Takuya Majima of Kyoto University for valuable comments and discussions. We also thank Masahiro Naitoh and Yoshitaka Sasaki of the accelerator facility of Quantum Science and Engineering Center, Kyoto University for technical support during the ion irradiation experiments. This work was supported by Kansai Atomic Energy Council.

References

[1] R. Wolfe and C. J. Kriessman, *Applied Solid State Science: Advances in Materials and Device Research*, Acadenic Press, New York and London, (1969).
[2] M. T. Myers, S. Charnvanichborikarn, L. Shao, and S. O. Kucheyev, Phys. Rev. Lett. **109**, 2 (2012).
[3] G. Carter, J. Appl. Phys. **79**, 8285 (1996).
[4] A. Hallén, D. Fenyö, B. U. R. Sundqvist, R. E. Johnson, and B. G. Svensson, J. Appl. Phys. **70**, 3025 (1991).
[5] A. I. Titov and G. Carter, Nucl. Instrum. Methods Phys. Res. Sect. B-Beam Interact. Mater. Atoms **119**, 491 (1996).
[6] H. Minagawa, H. Tsuchida, R. Murase, and A. Itoh, Nucl. Instrum. Methods Phys. Res. Sect. B-Beam Interact. Mater. Atoms **372**, 38 (2016).
[7] http://crystdb.nims.go.jp/.
[8] M. Hakala, M. J. Puska, and R. M. Nieminen, Phys. Rev. B **57**, 7621 (1998).

[9] C. A. J. Ammerlaan, H. Bracht, E. E. Haller, R. Murray, R. C. Newman, R. Sauer, N. A. Stolwijk, J. Weber, and W. Zulehner, Landolt Börnstein, New Series III/41A2α (2002).
[10] M. Trochet, L. K. Béland, J.-F. Joly, P. Brommer, and N. Mousseau, Phys. Rev. B **91**, 224106 (2015).
[11] G. S. Was, *Fundamentals of Radiation Materials Science: Metals and Alloys*, Second Edition, Springer-Verlag, Berlin, (2016).
[12] K. Nordlund, A. E. Sand, F. Granberg, S. J. Zinkle, R. Stoller, R. S. Averback, T. Suzudo, L. Malerba, F. Banhart, W. J. Weber, F. Willaime, S. Dudarev, and D. Simeone, Nuclear Science NEA/NSC/DOC 9 (2015).
[13] M. J. Norgett, M. T. Robinson, and I. M. Torrens, Nucl. Eng. Des. **33**, 50 (1975).
[14] A. Antonelli and J. Bernholc, Phys. Rev. B **40**, 10643 (1989).
[15] C. Wang, Z. Wang, and Q. Meng, Physica B **406**, 467 (2011).
[16] M. Tang, L. Colombo, J. Zhu, and T. Diaz de la Rubia, Phys. Rev. B **55**, 14279 (1997).
[17] J. A. Baker, T. N. Tucker, N. E. Moyer, and R. C. Buschert, J. Appl. Phys. **39**, 4365 (1968).